

Numerical Analysis for the Pressure Distribution along a Typical Fin-stabilized Missile

Mahmoud A. Moalla^{1*}, Sherif Saleh¹ and Mostafa Khalil¹

¹*Aerospace Engineering Department, Military Technical College, Cairo, 11776, Egypt*

*E-mail: m.abdelnaby.moalla@gmail.com

Abstract. Realizing the aerodynamic forces exerted on the missile structure for fin-stabilized missiles requires a good estimation of the pressure distribution along the missile body. This distribution has a direct impact on its structure, stability, and controllability, providing an essential pressure estimation to missile design. This study is performed by applying numerical calculations on a fin-stabilized missile with a slenderness ratio of 16.2. A detailed 3D model of the missile and its computational domain is constructed. The numerical simulations are performed by using the commercial software ANSYS Fluent. The results are validated with experimental wind tunnel data. The study has deep insight into how the pressure distribution along the missile airframe behaves at 4° and 8° angles of attack for Mach numbers 2 and 3.55. Finally, the effects of altitude impact on the pressure are also discussed, providing useful information on how the missile performs under different flight conditions.

1. Introduction

The analysis of pressure distribution over the missile airframe is essential for well understanding the aerodynamic forces exerted on its different sections. These forces have a direct impact on design parameters, including stability, control, and overall performance. Precise pressure measurements are essential for determining structural loads, aiding engineers in designing the missile airframe to be capable of withstanding the severe conditions of high-speed flight. Researchers in the open literature indicate that modeling airflow around missiles under varying flight conditions is crucial for comprehending pressure distributions along the missile airframe and the resulting aerodynamic forces. A study [1] developed numerical simulations, for missiles with square cross-sections to estimate the applied aerodynamic forces in various atmospheric conditions. These results were validated with experimental data for pressure distributed on the missile surface and the corresponding aerodynamic forces. Similarly, another study [2] had a good investigation on the impact of pressure distributions on the missile resulting from the nonlinear flow instabilities for missiles with elliptical cross-sections. Further study [3], proposed comprehensive datasets for pressure distributions, forces, and flowfields for supersonic missiles with high slenderness ratios. Various missile body cross-sectional configurations were analyzed [4] to demonstrate their aerodynamic properties and how pressure distribution affects the resulting aerodynamic efficiency. In addition [5] demonstrated the interaction between lateral jets and aerodynamic pressure distributions, as a validation done between the numerical simulations results and experimental data.

This paper gives a deep investigation of the pressure distribution around a typical fin-stabilized missile. Simulations are performed using the commercial software ANSYS Fluent [6]. The results are validated with available wind tunnel data. An analysis has been performed to examine the impact of the angle of attack (AOA) on the pressure distributions on the missile for Mach numbers 2 and 3.55. As well, the impact of the flight altitude on the resulting pressure differences is also investigated. The rest of this paper is organized as follows, next section, the case study, and

methodology are introduced. The main airframe configuration and dimensions are illustrated. Using experimental data from the literature, a validation case is presented comparing the pressure distributions along the missile. Finally, the results of numerical simulations performed are investigated.

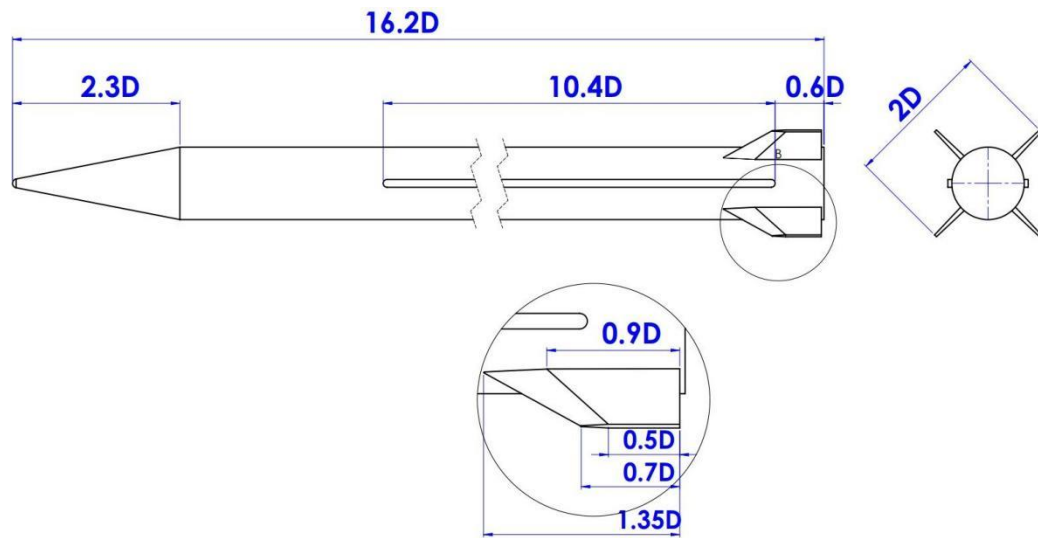


Figure 1. Fin stabilized missile with X-shape configuration.

2. Case study and Methodology

Through this study, a fin-stabilized missile with a slenderness ratio of 16.2 and four fin surfaces with an X-shape configuration, as shown in Figure 1, was utilized. A 3D model of the missile and its surrounding computational domain was created as illustrated in Figure 2. The domain dimensions were implemented to be sufficient for well capturing the aerodynamic flow phenomena such as shock waves and turbulent flow. An unstructured mesh was built using ANSYS Meshing as shown in Figure 3 considering the inner domain as a body of influence to ensure the refinement required for accurate prediction of aerodynamic behavior around the missile body with a cell count 16 millions.

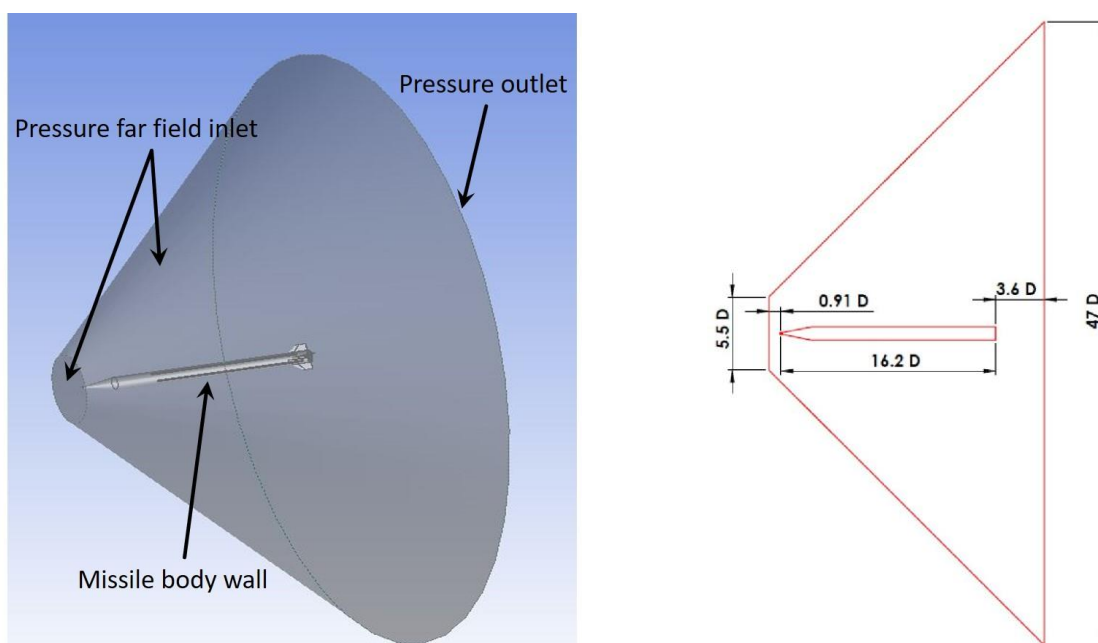


Figure 2. 3-D model for the case study and computational domain.

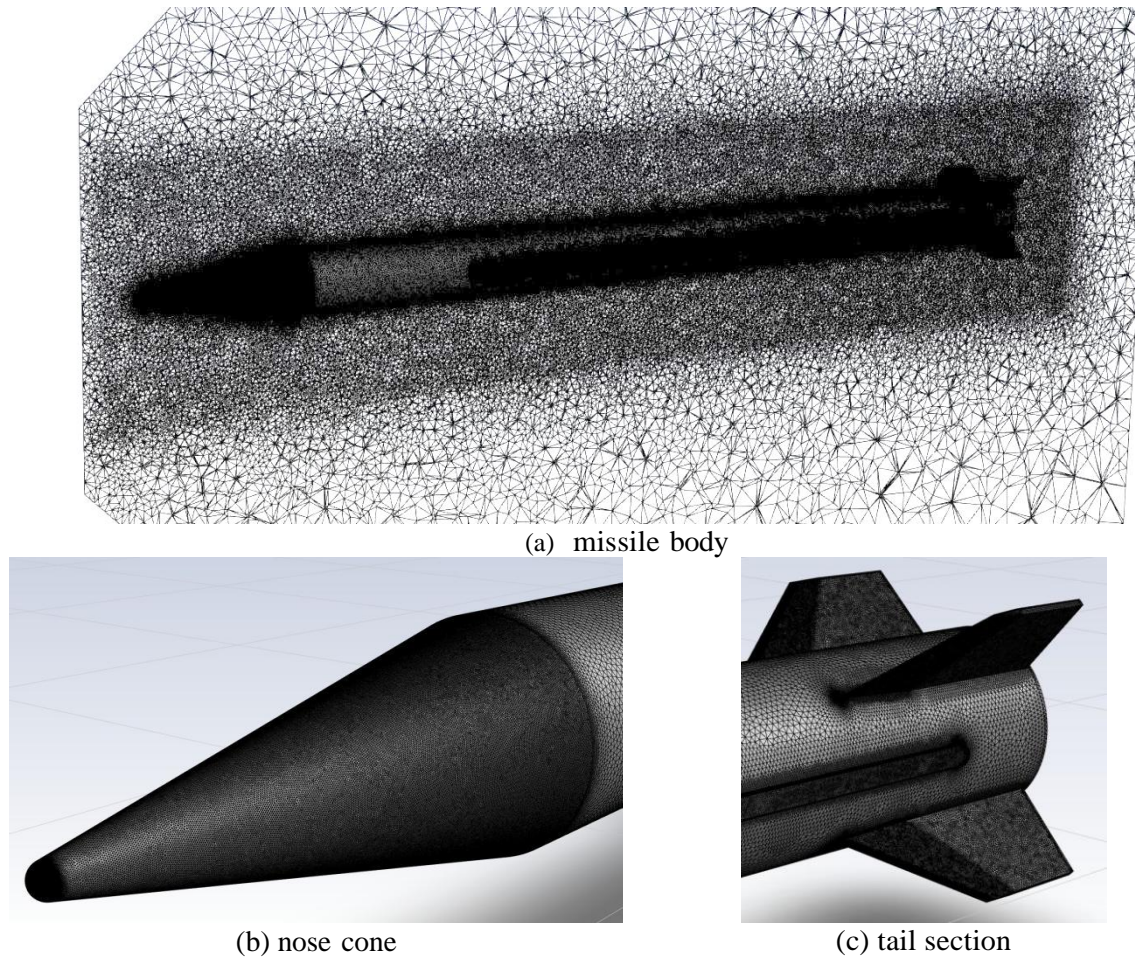


Figure 3. Unstructured mesh for the computational domain.

ANSYS Fluent was used in this study as a powerful tool for Computational Fluid Dynamics (CFD) simulations, which is very suitable for complicated cases just as simulating the airflow around a fin-stabilized missile. Fluent's density-based solver [7] [8] is used because it is well suitable for handling high-speed, compressible flows like those involving supersonic speeds and shock waves. The Shear Stress Transport (SST) $k-\omega$ turbulence model [9] [10] as it provides well-accurate predictions of how airflow behaves, especially in spaces where the airflow may be separated from the surface as well as in high-speed conditions. For the setup of the simulation, pressure far-field condition was applied at the inlet of the domain to give a good representation of the freestream properties like Mach number and static pressure. For the flowfield domain outlet, a pressure condition is used to allow airflow to exit the domain smoothly. The governing equations were solved by using a "second-order upwind scheme" taking about 480 hours solving time.

3. Results and discussion

3.1. Validation case

For a validation purpose, ten locations along the missile body were selected to estimate the pressure coefficient (C_p) numerically compared with the experimental wind-tunnel data (WT) done by the research group. The validation was performed under particular conditions, with a Mach number of 2 and 4° angle of attack. In numerical simulations, C_p values were estimated at the stagnation point and the other ten locations were distributed along the missile body length (L) at both upward and downward sides. These measurement points are located at $x/L = 0.1, 0.14, 0.15, 0.17, 0.21, 0.28, 0.47, 0.65, 0.87$, and 0.96 .

As illustrated in Figures 4 C_p values estimated (CFD) against the wind tunnel values (WT) show a good agreement representing that the numerical simulations accurately represent the missile aerodynamic behaviors, including the missile nose stagnation pressure and the pressure distribution along the missile surface. This agreement highlights the reliability of the CFD model for simulating the missile's aerodynamic performance.

Additional analyses are provided in Figure 5, representing the C_p distribution around the missile cross-section at three subsequent locations along its length, namely at $x/L = 0.1, 0.14$, and 0.15 . Section 1 (S1), almost at the middle of the cone, Section 2 (S2), just before the cone-cylinder transition, and Section 3 (S3), just after the cone-cylinder transition.

As shown in S1, Figure 5(a), a smooth pressure gradient is observed as the pressure gradually decreases from the downward side to the upward one. In S2, a similar contour gradient is presented along the missile nose length as illustrated in Figure 5(b). This reflects a consistent pressure distribution along the missile conical nose. However, the transition between the nose and cylinder, shown in S3, introduces a strong pressure gradient on the downward surface toward the upward surface. Flow separation zone on the most upward region is presented, resulting in higher pressure difference leading to high contribution on the missile lift. These findings conclude the critical role of transition geometry in contributing to aerodynamic performance.

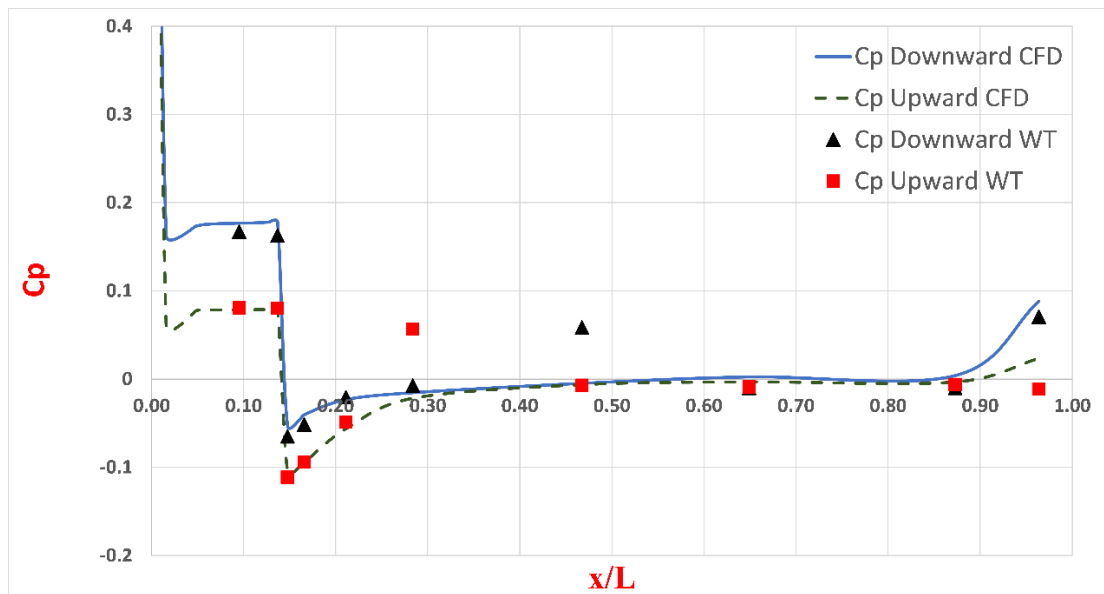


Figure 4. Downward pressure coefficient C_p along missile body (x/L) for $M = 2$ and $\alpha = 4^\circ$.

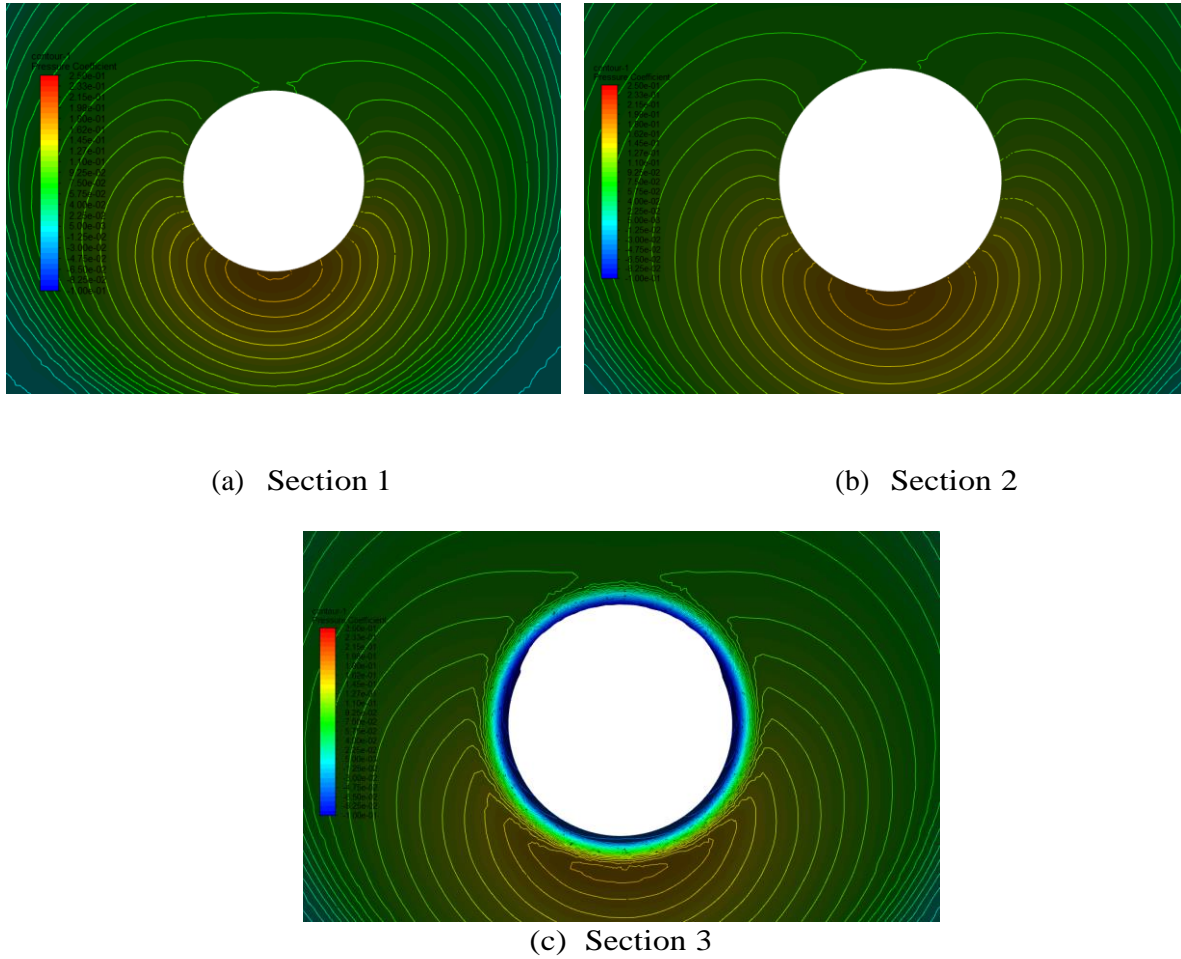


Figure 5. Pressure coefficient C_p at $\alpha = 4^\circ$ and $M = 2$

3.2. Impact of Flight Conditions.

3.2.1. Impact of Mach Number

To study how changes in Mach number affect the pressure distribution along the missile body, simulations were performed at AOA $\alpha = 4^\circ$ for Mach numbers 2 and 3.5, as shown in Figure 6. Additional details are provided in Figure 7, where the C_p distribution around the downward surface of the missile at three subsequent cross-sections, S1, S2, and S3 are illustrated. The analysis shows that as the Mach number increases, the C_p decreases noticeably. This trend is primarily due to compressibility effects, which intensify at higher speeds near and beyond supersonic levels, however, it can be noticed that in section 3 the values of C_p for $M = 3.5$ are higher than the values for $M = 2$. Due to the impact of the presence of the cone-cylinder transition, as shown in Figure 8, a wake region is observed downstream of this transition for $M = 2$, however, for $M = 3.5$, this wake region vanished due to the stronger shock wave generated at higher Mach numbers. The stronger shock wave prevents the airflow from an extreme decrease in the pressure coefficient C_p through the expansion fan.

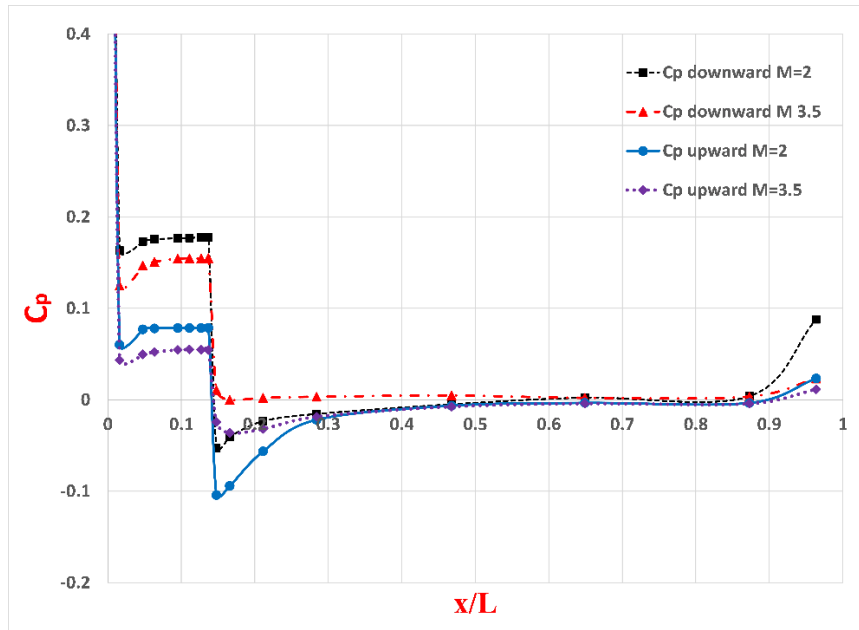
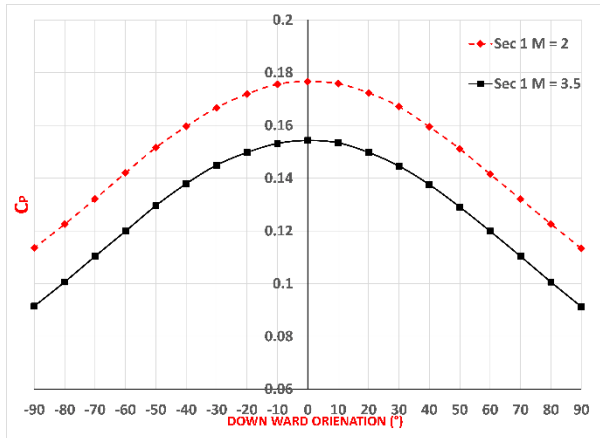
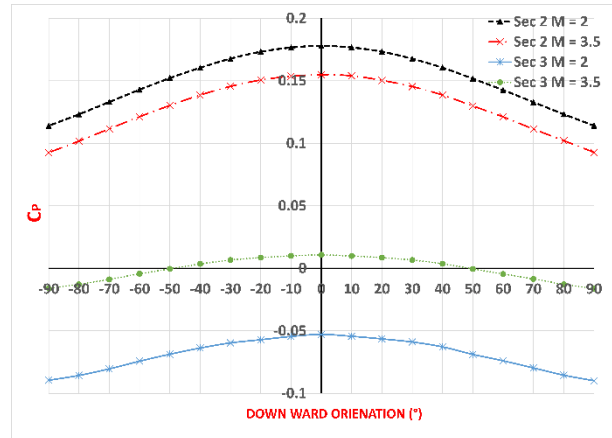


Figure 6. Pressure distribution along the missile body at $\alpha = 4^\circ$

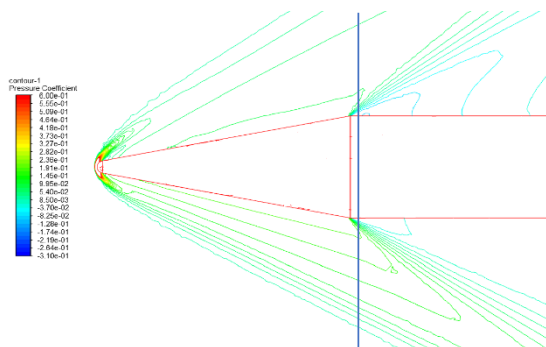


(a) at $x/L = 0.1$

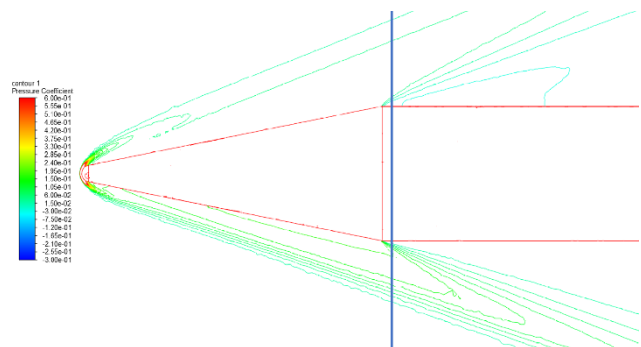


(b) at $x/L = 0.14$ and 0.15

Figure 7. Pressure coefficient C_p for downward orientation for $\alpha = 4^\circ$



(a) at $M = 2$



(b) at $M = 3.5$

Figure 8. Pressure coefficient C_p contours at cone-cylinder transition for $\alpha = 4^\circ$

3.2.2 Impact of Angle of Attack

Simulations were performed at Mach 2 for two angles of attack, namely 4° and 8° , as illustrated in Figure 9, showing the variation in the pressure coefficient C_p along the missile length. It can be concluded that as the AOA increased the pressure difference between the missile downward and upward surfaces increased increasing the resultant lift force on the missile.

Additional visualizations, for pressure distribution along the downward surface at the three locations, namely S1, S2, and S3, are shown in Figure 10. For the downward-facing side of the missile, the C_p values increased with increasing AOA. Additionally, a stronger pressure recovery along different missile cross-sections is presented.

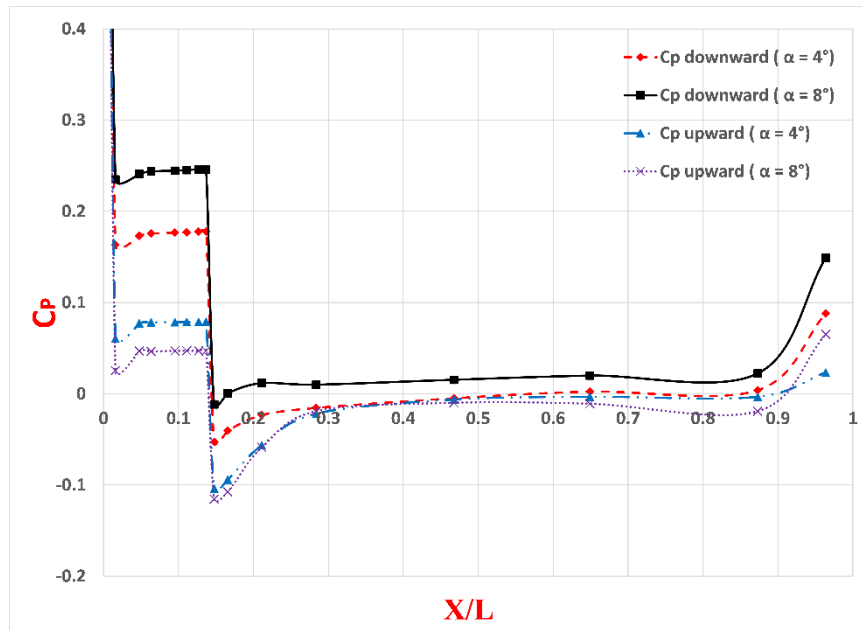


Figure 9. C_p distribution along the missile body at $M = 2$.

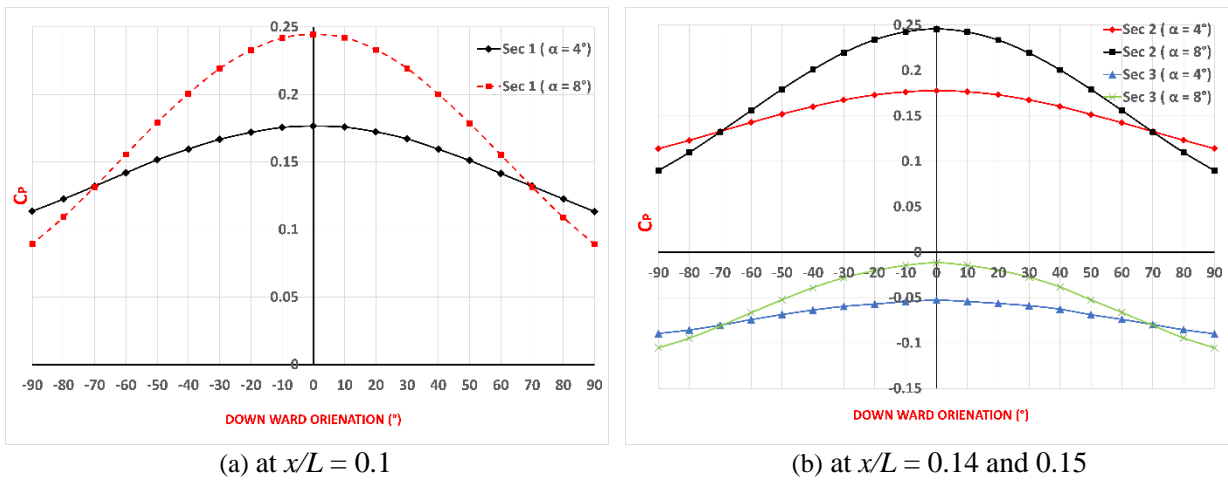


Figure 10. pressure coefficient C_p for downward orientation at $M = 2$

Examining the pressure around different sections, the pressure distribution in S1 shows higher values observed on the downward facing as AOA increased, where a sharper pressure gradient was revealed compared to the lower AOA case. At S2, the same pressure gradient is obtained as S1 representing that the pressure gradient along conical nose shapes is almost zero, as illustrated in Figure 10. Finally, it can be concluded that a more pronounced aerodynamic response to the AOA change was attained.

Table 1. Atmospheric conditions for different geometric altitudes at Mach 2.

Altitude (km)	Air Density (kg/m ³)	Velocity (m/s)	P_{dyn} (bar)
0	1.225	680.6	2.0
5.5	0.69711	636.98	2.84
35	0.00816	619.24	0.02

3.2.3 Impact of Altitude

This analysis examines how altitude changes affect the static pressure distribution along the missile body for flight conditions Mach 2, 4° AOA, and different altitudes, namely sea-level, 5.5 km, and 35 km. Firstly, applying the international standard atmosphere [11], the air density and sonic speed are calculated at different geometric altitudes. As listed in Table 1, the dynamic pressure is calculated, and the corresponding static pressure is obtained as,

$$C_p = \frac{P - P_\infty}{P_{dyn}}$$

The results show that as the geometric altitude increased the dynamic pressure (P_{dyn}) for the same Mach number decreased. This behavior may happen due to reduced air density for higher altitudes. This finding indicates that as altitude rises, the pressure distribution along the missile body decreases, as illustrated in Figure 11.

These results highlight the significant influence of altitude on pressure distribution, which is critical for understanding aerodynamic loads and designing missile structures for varying atmospheric conditions.

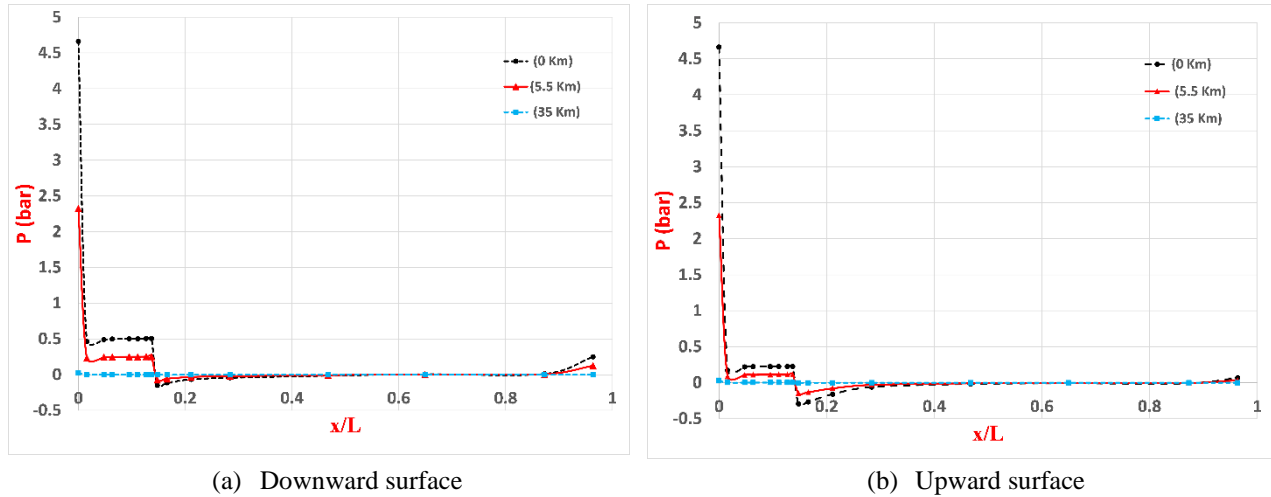


Figure 11. Static Pressure distribution along the missile body for $M = 2$ and $\alpha = 4^\circ$.

4. Conclusion

This study offers an aerodynamic analysis of a missile body under varying flight conditions, focusing on how Mach number, angle of attack, and altitude influence pressure distributions. The study uses computational fluid dynamics (CFD) and started by validating the model with wind tunnel data. An excellent agreement was shown between the CFD-predicted pressure coefficients (C_p) and experimental results, which validated the reliability of the CFD model in predicting complex aerodynamic phenomena. Important features such as stagnation pressure and pressure recovery along the missile body were accurately represented, demonstrating the robustness of the numerical model. The analysis of Mach number effects revealed that as the Mach number increases, C_p values decrease due to stronger compressibility effects and sharper shock waves. The study also analyzed the influence of the AOA change, showing that higher angles of attack result in increased pressure recovery on the downward side of the missile, while the upward side experiences reduced static pressure due to lower flow deflections. This pressure difference generates higher pitching moments and lift forces, which are essential in missile structure calculations. Altitude effects were analyzed, with results indicating that pressure decreases with increasing altitude due to reduced air density. In summary, this study explores the complex interactions between Mach number, angle of attack, and altitude in determining aerodynamic performance. The findings provide valuable insights into missile aerodynamics. Future research could build on this work by using this model as a sub-module in a fluid-structure interaction model to study the influence of high speeds on missile structure, especially for maximum dynamic pressure conditions.

References

- [1] Floyd J. Wilcox, Jr. 2004 *Force, Surface Pressure, and Flowfield Measurements on a Slender Missile Configuration with Square Cross-Section at Supersonic Speeds* NASA Technical Report (<https://ntrs.nasa.gov>)
- [2] Jerry M. Allen and 1983 *Analysis of Surface Pressure Distributions on Two Elliptic Missile Bodies* NASA Technical Report (<https://ntrs.nasa.gov>)
- [3] Trevor Birch 2000 *Force, Surface Pressure, and Flowfield Measurements on Slender Missile Configurations at Supersonic Speeds* NASA Technical Report (<https://ntrs.nasa.gov>)
- [4] Nathan Shumway 2023 *Experimental and Numerical Comparison of Different Missile Body Cross Sectional Shapes* Edlib International Conference Proceedings (<https://www.edlib.net>)
- [5] Patrick Gnemmi 2008 *Computational Comparisons of the Interaction of a Lateral Jet on a Generic Supersonic Missile* AIAA 26th Applied Aerodynamics Conference Proceedings (<https://elib.dlr.de>)
- [6] ANSYS® Fluent, Release 2020 R1, Help System, ANSYS Inc., Canonsburg, PA, USA.
- [7] Kim J, et al. 2022 An automated aerodynamic analysis system in missile based on open source software *Int. J. Aeronaut. Space Sci.* **24**, 592–605 (2023). (<https://link.springer.com/article/10.1007/s42405-022-00558-0>)
- [8] Singh A K, et al. 2007 Simulation of external hypersonic problems using FLUENT 6.3 density-based solver *European Conference on Computational Fluid Dynamics* Available: <https://www.eucass.eu/component/docindexer/?id=2832&task=download>
- [9] Rumsey C L 2010 *Compressibility Considerations for $k-\omega$ Turbulence Models in Hypersonic Boundary-Layer Applications* NASA Langley Research Center
- [10] Pang A L J, Skote M and Lim S Y 2016 Modelling High Re flow around a 2D cylindrical bluff body using the $k-\omega$ (SST) turbulence model *Progress in Computational Fluid Dynamics* **16**(1) 48–57
- [11] National Aeronautics and Space Administration (NASA), 1976, 'US Standard Atmosphere 1976', NASA Technical Paper 4111, available at: <https://ntrs.nasa.gov/citations/19770009539>.